

Rapid sea level rise causes loss of seagrass meadows

Kyle A. Capistrant-Fossa¹   & Kenneth H. Dunton¹

As global declines in seagrass populations continue to cause great concern, long-term assessment of seagrass meadows show promise in furnishing valuable clues into fundamental causes of seagrass loss and drivers of environmental change. Here we report two long-term records of seagrass presence in western Gulf of Mexico coastal waters (Laguna Madre) that provided insight into their rapid decline in a relatively pristine ecosystem. Coincident with unprecedented increases in water depth starting in 2014 ($14\text{--}25\text{ mm y}^{-1}$), monthly measurements at a deep edge fixed station revealed that two ubiquitous seagrass species (*Halodule wrightii* and *Syringodium filiforme*) vanished altogether in just five years; a subsequent basin-wide assessment revealed that seagrasses disappeared at 23% of 144 sentinel stations. Models that incorporate differing sea level rise scenarios and water depth thresholds reveal potential global losses of seagrass habitat ($14,000\text{ km}^2$), with expansion into newly created shallow habitats constrained by altered natural shorelines.

¹The University of Texas at Austin, Marine Science Institute, Port Aransas, USA. ✉email: kyle.capistrantfossa@utexas.edu

Seagrasses, a polyphyletic group of angiosperms containing over 60 species, possess specialized adaptations for aquatic life that have facilitated colonization across 160,000 km² of coastal ecosystems^{1,2}. Common environmental conditions such as temperature, salinity, predation, nutrients concentration, and light availability are often identified as major controls of seagrass abundance and spatial distribution^{3,4}. As a well-recognized foundation species, seagrasses provide numerous ecosystem services valued at over \$19,000 ha⁻¹, including nursery habitat for fisheries, food for numerous marine organisms, shoreline protection, ecotourism, and educational opportunities^{5,6}. The role of seagrass within earth's global carbon biochemical cycle is becoming increasingly recognized due to their high productivity and sequestration of allochthonous and autochthonous blue (organic) and inorganic carbon in sediments^{7–9}. Seagrasses contain a disproportionately high carbon stock (0.025 Tg km⁻²) compared to high-biomass terrestrial forests (0.014 Tg km⁻²) and are able to potentially store this carbon for thousands of years if undisturbed^{10–12}.

Despite the global importance of seagrass meadows, their persistence is significantly threatened due to a variety of factors¹³. Since the mid-1700s, the global coverage of seagrasses has decreased by about 29% (51,000 km²) with 10 species at risk of extinction^{14,15}. Furthermore, annual losses of seagrass habitat return about 300 Tg C y⁻¹ to the global active carbon pool¹⁰. Major anthropogenic and environmental drivers of seagrass loss include algal blooms¹⁶, chemical pollution¹⁷, disease¹⁸, drought^{19,20}, eutrophication²¹, heat waves²², invasive species²³, mechanical damage²⁴, and storm action²⁰. Mechanistically, these drivers disrupt the plant's photosynthetic balance between carbon fixation and respiration by (1) limiting the light available for photosynthesis, (2) altering the basal metabolic costs of the plant, and/or (3) damaging the plant's photosynthetic apparatus. Seagrasses have one of the highest light requirements of aquatic photoautotrophs owing to the high respiratory demand of their root/rhizome system, which must maintain an oxidized rhizosphere in an otherwise anoxic environment^{25,26}.

Seagrass meadows persist at a variety of depths (0–90 m), but species-specific tolerances to light availability control community composition along this steep gradient²⁵. Plants living near the edge of their physiological light limit maintain a neutral to slightly positive carbon balance and are known as deep edge populations. In aquatic environments, irradiance at depth (I_z) is modelled using the equation $I_z = I_0 e^{-K_d z}$, where I_0 is surface irradiance, z is depth, and K_d is the extinction coefficient. Typical values of K_d in pristine western Gulf of Mexico estuaries (e.g., Laguna Madre²⁷) range between 1 and 2, with a change of 0.1 m sufficient to reduce bottom irradiance by 10–20%. Consequently, slight changes in water depth may impact the ability of the populations to persist, which allows them to act as sentinel species for long-term shifts in water depth.

Over the past century, global mean sea level has increased by 1–3 mm y⁻¹ depending on a suite of complex factors including subsidence, crustal uplift, isostatic rebound, thermal expansion, and glacial melt runoff²⁸. In contrast, recent cycles of Rossby waves have increased rates of sea level rise (SLR) in the Gulf of Mexico²⁹, a region already rising 2–3 times faster than the global average³⁰, to >10 mm y⁻¹ since 2010. Numerous local factors can amplify these effects as exemplified by the weight of water displaced during Hurricane Harvey, which depressed coastal regions of Texas by up 20 mm for weeks after the storm³¹. Likewise, water and hydrocarbon extraction are causing land subsidence of up to 9.5 mm y⁻¹ within the Texas Coastal Bend³². As water depths increase, seagrass distribution may shift away from deeper waters and begin to colonize newly submerged lands. However, an increasing fraction (14% and growing) of US shorelines are hardened³³ to protect from coastal hazards (e.g., groins, jetties, breakwaters), preventing

seagrass proliferation into shallow waters and leading to a net loss of habitat.

Turbid coastal waters threaten seagrass meadow persistence because SLR-driven light loss compounds natural attenuation processes. Here, we classify a habitat as “turbid” if $K_d > 1$ (i.e., over 33% greater than the global average) and is representative of areas with low water clarity (e.g., Baltic Sea, Laguna Madre, West Florida Shelf)^{27,34,35}. Resource managers have developed numerous regional models to project distributional changes in seagrass cover under varying scenarios of SLR, K_d , and eutrophication across the globe^{36,37}. Recent advances in mathematics and statistics have enabled some models to accurately predict if SLR will cause the environment to become hydrodynamically unfavorable³⁸. Previous experiments have focused on addressing similar mechanisms to SLR (i.e., in-situ light reduction)¹⁶, but do not represent realistic conditions. For example, intertidal *Zostera japonica* grew better under simulated SLR conditions³⁹ and seagrasses experienced both areal losses and gains following localized crustal subsidence in the Solomon Islands⁴⁰. Contemporary rates of SLR require long-term seagrass monitoring projects to properly document evidence of change. To date only one seagrass monitoring program has hypothesized SLR caused the retreat of deep-edge seagrasses (*Posidonia oceanica*)⁴¹; however, they were unable to disentangle results from natural climate oscillations. The present study uses two independent long-term seagrass monitoring datasets synergistically to verify that sea level rise is causing a significant contemporary loss of seagrasses over an enormous spatial extent.

Here we examine two long-term records of seagrass presence in the Upper Laguna Madre (TX, USA) to investigate the rapid decline of seagrasses in a relatively pristine ecosystem: a fixed deep edge station (LM-151) and basin-wide sampling of 144 sentinel Tier-2 stations (Fig. 1). Our monitoring at deep edge station LM-151 documented the recent disappearance of seagrasses from this area after 30 years of monitoring. By combining data from these two programs, we noted that vegetation shifts at LM-151 (sampled at monthly intervals for three decades) were confirmed on a landscape scale at our 144 sentinel stations sampled annually over the period 2011–2022. We hypothesize that seagrass losses at the deep edge site were caused by long-term increases in water depth and that rises in water level were also responsible for seagrass loss on a landscape scale at deeper edge populations throughout the Upper Laguna Madre.

Results

Environmental Conditions. Water temperature varies seasonally at LM-151 with hot summers (max = 34 °C) and cooler winters (min = 7.8 °C) with relatively low interannual variability (Fig. 2a). In contrast, average daytime underwater irradiance (ADI), water depth, and salinity have strong intra- and inter-annual variability (Fig. 2b, c, Figure S1). Irradiance was lowest in the early 1990s, increased and plateaued from 2000 to 2015 before beginning to decline to its lowest levels since measurements began in 1989 (Fig. 2b, Figure S2). Salinity varied among years (Figure S1) but rapidly switched in the early 2010s from a hyposaline (17) to a hypersaline environment (62.6). Water depth increased in 1990s, decreased in the 2000s, and has significantly ($p = 0.02$) increased since 2014 by 14 mm yr⁻¹ (Fig. 2c). Across the Texas coast similar patterns were found with low rates of sea level change pre-2014 (up to 9 mm y⁻¹), followed by a significant increase afterwards (3–21 mm y⁻¹; Fig. 2d). Low water depths in the 2010s corresponded with increased Secchi depth, decreased TSS, and decreased pH within the water column (Figure S1). Dissolved oxygen, ammonium and dissolved inorganic nitrogen remained relatively constant until the late 2010s while DO decreased and DIN and

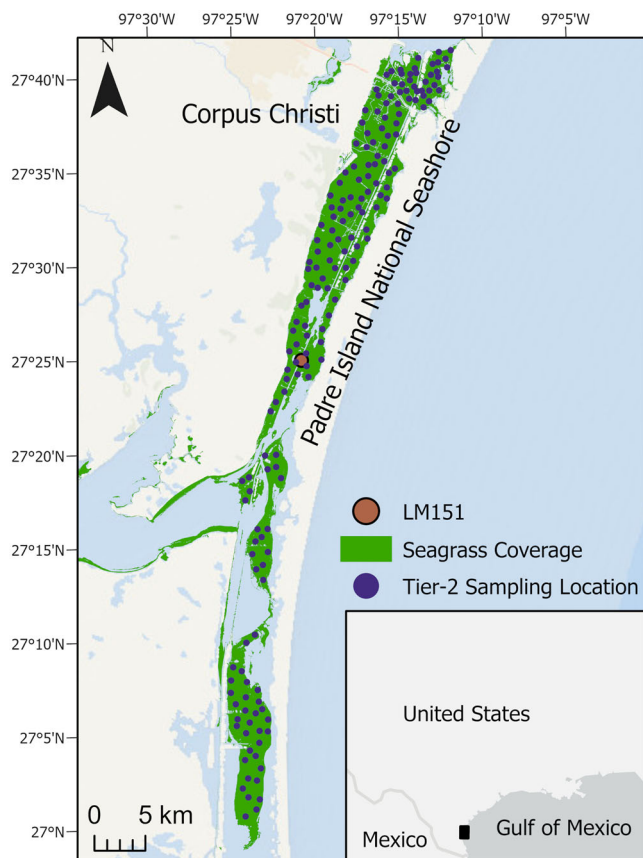


Fig. 1 Seagrass monitoring locations within the Upper Laguna Madre (TX, USA). Seagrass coverage represents historically known meadows within the system⁵⁷. The brown closed circle is the LM-151 station while the purple closed circles are Tier-2 sampling sites.

NH_4^+ significantly increased (Figure S1). Algal epiphytes are constant at LM-151 throughout time and are lower than other monitoring stations along the Texas coast (Figure S1).

Tier-2 sentinel sites formed five distinct clusters based on water depth measurements during annual monitoring from 2011 to 2022 (Fig. 3). Cluster 4 had the lowest average water depth (0.45 m) whereas Cluster 5 had the highest (1.66 m). There was relatively low variability in depth between Cluster 1 (0.75 m), Cluster 2 (0.96 m), and Cluster 3 (1.22 m). Overall, the interannual water depth variability at each site was fairly low, but many sites in Cluster 1 were characterized by high variability.

Biological parameters. From 1989 to 2005 LM-151 was nearly a monotypic *Halodule wrightii* meadow, but in 2005 *Syringodium filiforme* recruited, and by the early 2010s had greater biomass than *Halodule* and equal density (Fig. 4a, b, d). *Syringodium* then retreated and was completely absent by 2013, but *Halodule* did not return to its pre-2010 levels. By 2018 *Halodule* also disappeared from the site. Biomass ratios revealed *Syringodium* lost aboveground tissues before belowground, whereas the opposite was true for *Halodule* (Fig. 4c).

Seagrass was present during annual Tier-2 monitoring from 2011 to 2022 at most monitoring stations (left panel Fig. 3), but varied amongst sites grouped by water depth. Cluster 5 (deepest sites) lost most seagrass. In 2013 seagrass was present at 80% of Cluster 5 sites, dropping precipitously to 4% by 2022 (Fig. 3). Overall, Cluster 2 (intermediate depths) had the highest proportion of seagrass presence during sampling (259/261 samplings), whereas Cluster 5 had the lowest (130/261 samplings).

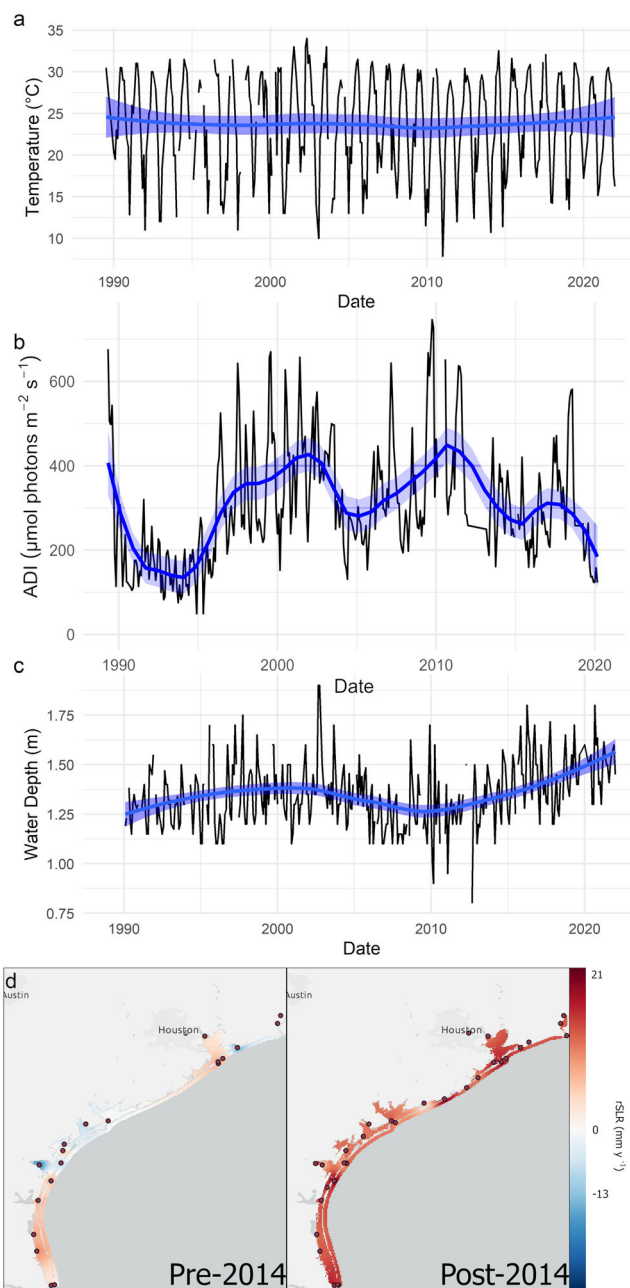


Fig. 2 Environmental variables from LM-151. **a–c** Variations in temperature, average daytime irradiance (ADI), and water depth. **d** Calculated rates of relative sea level rise from NOAA buoys before or after 2014. Black data represents observations while blue lines represent the results of LOESS smoothing; shaded region is the standard error.

Relationship between seagrass and environment. Water temperature and bottom irradiance were significant predictors of both *Syringodium* ($R^2 = 0.68$) and *Halodule* ($R^2 = 0.31$) aboveground biomass (Table S1) at LM-151, but water depth and irradiance best explained the presence of *Syringodium* ($R^2 = 0.22$). *Syringodium* biomass had narrower optimal environmental conditions ($25\text{--}30^\circ\text{C}$, $\geq 365 \mu\text{mol photons m}^{-2} \text{s}^{-1}$; Figure S3a) than *Halodule* ($\geq 25^\circ\text{C}$, $\geq 50 \mu\text{mol photons m}^{-2} \text{s}^{-1}$; Figure S3c). However, both *Syringodium* and *Halodule* were negatively influenced by high light under cooler conditions (Figure S3a). Overall, *Syringodium* was less likely to be present at LM-151 under dim, deep conditions ($\leq 200 \mu\text{mol photons m}^{-2} \text{s}^{-1}$ and $\geq 1.5\text{ m}$)

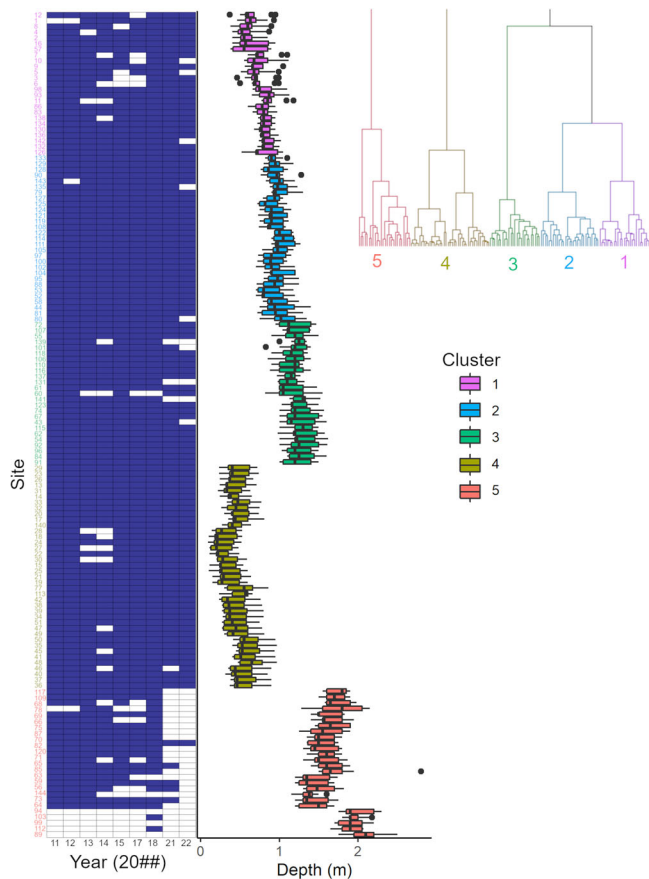


Fig. 3 The presence (blue shading) or absence (white shading) of seagrass at Tier-2 monitoring stations. Sites and colors are aligned based off hierarchical cluster of water depth measurements. The inset shows the overall clustering scheme with clusters 4 + 5 different from 1 to 3. Boxplots represent the distribution of collected water depth data at each monitoring station with individual points falling outside the 95% confidence interval.

Seagrass presence at Tier-2 sampling sites was significantly affected by water depth, year, and the site's geographic coordinates ($R^2 = 0.62$; Table S1). Generally, water depths greater than 1.5 m negatively affected the probability of seagrass presence, but the strength of this effect varied among years (e.g., 2017–2018; Figure S3d). Spatially, seagrasses were more likely to be found in northeastern Laguna Madre, and least likely in the southern region (Figure S4).

Seagrass meadows have historically covered up to 200 km² within Upper Laguna Madre, but by 2018 suitable seagrass habitat decreased by more than 41 km² with the increased prevalence of water depths ≥ 1.5 m (Fig. 5). Under varying sea-level rise scenarios, this unsuitable habitat will expand to 73–113 km², especially within the northern reaches of the estuary. However, newly submerged habitat is predicted to vary between 90 and 135 km², creating a potential net gain of 59–65 km² in suitable seagrass habitat.

Discussion

This study synthesizes decades of monitoring efforts (LM-151 & sentinel Tier-2 stations) to assess the long-term response of seagrass populations at local and landscape scales to environmental changes within the Upper Laguna Madre. Over the past 30 years *Syringodium* and *Halodule* populations showed a typical successional pattern at a deep edge monitoring station (LM-151), but overall seagrass cover began to decline significantly after 2014 as sea level continued to rapidly rise at a rate of 14 mm y⁻¹.

Statistical modeling revealed that seagrass biomass was sensitive to changes in temperature and bottom irradiance, whereas seagrass presence was controlled by water depth and irradiance. Since 2018 seagrass has vanished from the LM-151 deep edge site and from deep Tier-2 monitoring locations across the Upper Laguna Madre.

Halodule wrightii and *Syringodium filiforme* are both common subtropical Atlantic species but have varying biological characteristics that lead them to represent different successional stages. At LM-151, *Halodule* populations thrived until 2007; at that time *Syringodium* began to invade and shade the shorter *Halodule* canopy. *Halodule* is typically a pioneer species that has faster growth rates, higher nutrient requirements, and is more tolerant of hypersaline conditions than *Syringodium*^{42,43}. The sudden decline of *Syringodium* in 2012 was caused by drought-induced hypersalinity⁴⁴. We would expect *Syringodium filiforme* biomass to have a stronger correlation with the environment than *Halodule wrightii* because it has more specific growth requirements. Indeed, we found a greater link with *Syringodium* ($R^2 = 0.68$) and environmental conditions than *Halodule* ($R^2 = 0.31$). However, both species were tied to the same environmental variables that often control seagrass annual biomass cycles: water temperature and irradiance^{3,4,44,45}.

In the absence of no significant long-term and consistent trends in temperature or salinity, we believe that low irradiance is responsible for the slow disappearance of seagrasses since 2014. This includes the failure of *Syringodium* to recolonize as salinities moderated, the slow disappearance of *Halodule* at LM-151, and the overall loss of seagrasses throughout the Upper Laguna Madre. Continuous records of irradiance at LM-151 depict a nearly steady decline in PAR since 2012, coincident with rising water levels. By spring 2020 average daily irradiance had reached their lowest levels since the early 1990s when a chrysophyte (brown tide) algal bloom resulted in a rapid (six-month) decline in irradiance⁴⁶. Bare spots formed in deep edge *Halodule wrightii* meadows of ULM (1.4 m) two years post-light reduction from this event²⁷. The magnitude of contemporary seagrass loss from relative sea level rise is similar to the multi-year effects of the brown tide algal bloom highlighting the need for adaptive environmental regulations because of shifting environmental baselines.

Partial effect plots generated through general additive modeling (Figure S3) are valuable tools for identifying physiologically relevant drivers of seagrass distribution. For example, we identified optimum *Syringodium filiforme* conditions between 25 and 30 °C and ≥ 365 $\mu\text{mol photons m}^{-2} \text{ s}^{-1}$. Previous research identified that peak productivity occurred between 23 and 29 °C⁴⁷ and photosynthesis became saturated⁴⁸ at 370 $\mu\text{mol photons m}^{-2}$. Likewise, *Halodule* biomass increased at ≥ 25 °C water temperature across all measured irradiances. These values agree with regional measurements of optimal water temperatures (25–30 °C)⁴ and saturation (100–600 $\mu\text{mol photons m}^{-2}$ depending on the season)⁴⁵. Together, these results suggest that the individual physiologies of the plants are more important in shaping the communities than physical disruption from local climatic events (e.g., storms or freezing).

Changes in the below:aboveground biomass ratio yield insight into the drivers of seagrass loss. The ratio rapidly rises as *Syringodium* photosynthetic tissues are lost to the system, indicating an acute stress. Depending on the duration, recovery from belowground tissues (roots/rhizomes) is possible. Earlier work described widescale *Syringodium* loss in Laguna Madre in 2011 and 2012 because of drought-induced hypersalinity⁴⁴, but *Syringodium* has not returned to LM-151 despite salinity decreases. Conversely, the below:aboveground biomass ratio in *Halodule* is known to decline slightly in response to chronic stressors that reduces the plant photosynthetic output or increases their basal metabolic costs⁴⁹. Likewise, *Halodule uninervis* had a significant

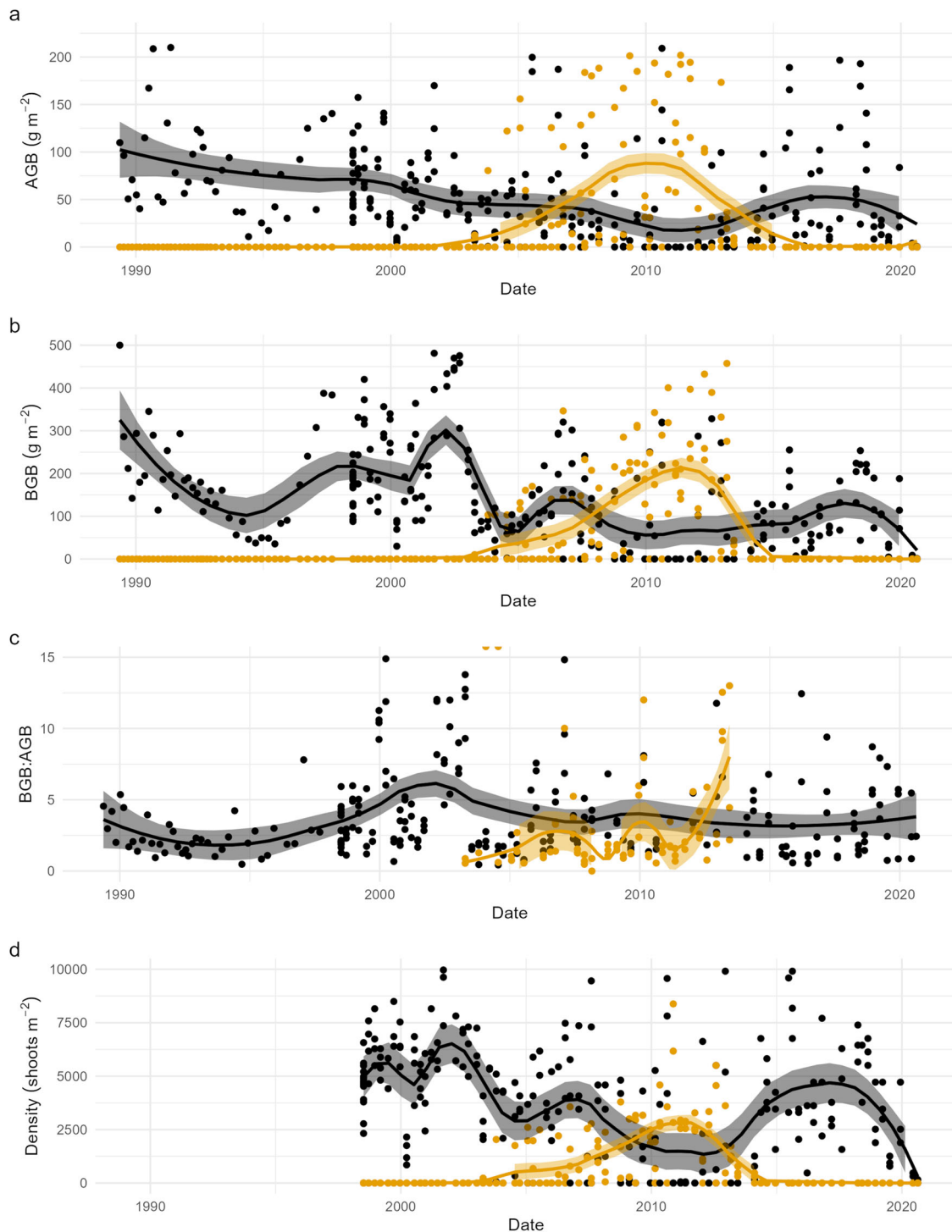


Fig. 4 Seagrass biomass metrics measured at LM-151 from 1989 to 2022. **a** Aboveground biomass, **b** Belowground biomass, **c** Belowground: aboveground biomass ratios, and **d** Shoot density. Black represents *Halodule wrightii* and orange represents *Syringodium filiforme*. Lines represent the results of LOESS smoothing; shaded region is the standard error.

reduction in biomass, but maintained a constant root:shoot ratio during a year of shading⁵⁰. The long-term decline of seagrasses in Indian River lagoon shows a similar pattern⁵¹. Therefore, an added stressor beyond salinity likely prevented recolonization of *Syringodium* and caused a *Halodule* decline.

We do not believe eutrophication was a major cause of seagrass loss at LM-151 because nutrient spikes occurred following seagrass loss in the Upper Laguna Madre. Increases in nutrient concentrations are attributed to both the loss of seagrasses as a

significant sink of dissolved inorganic-N^{52,53} and benthic remineralization of increased seagrass derived organicized matter as plants slowly died. Additionally, decreases in water column oxygen concentration coincided with seagrass biomass decline. There is no evidence of eutrophication since the monitoring stations fall within the bounds of an undeveloped national park and there are no changes in epiphyte loading over the past decade (Figure S1). We found a strong negative relationship between water depth and seagrass biomass in Laguna Madre. Long-term

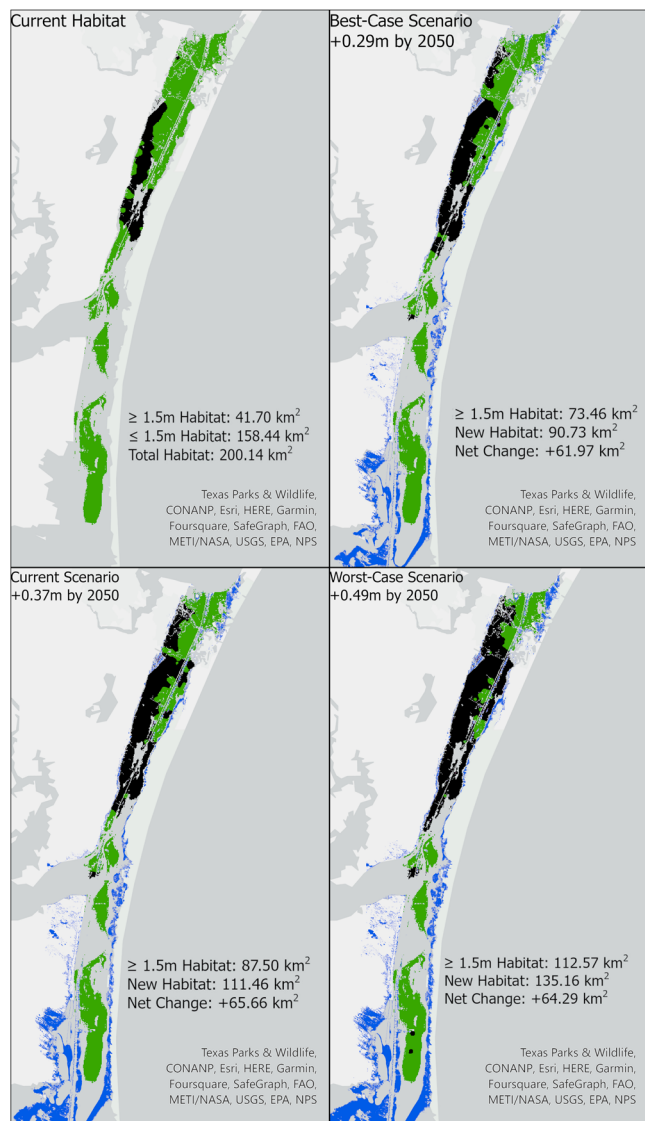


Fig. 5 Potential seagrass distribution under current and future sea-level rise scenarios. Green represents areas at <1.5 m water depth (potential seagrass habitat), black at ≥ 1.5 m water depth (not suitable for seagrasses), and blue as newly submerged seafloor.

changes in water level would function as a chronic stressor that integrates various environmental factors (e.g., stratification, temperature), but especially light penetration.

Contributions from thermal expansion of rapidly warming waters as well as large removals of groundwater produce a rate of relative sea level rise (rSLR) along Texas' Gulf Coast that is one of the highest in the world^{29,30}. Water depth data collected for over 100 yr in Galveston (TX, USA) revealed a rSLR rate of 6.6 mm y^{-1} , nearly 3x faster than the global average³⁰. Here we report contemporary (post-2014) water-depth increases far exceeding this average at 28 out of 31 NOAA stations (up to 21 mm y^{-1} in Nueces Bay) and our long-term LM-151 site. In contrast, 14 out of 20 stations had rates lower than 6.6 mm y^{-1} from 1990 to 2013. Our calculated rSLR rates may over predict true rates because the NOAA data are referenced to a geodetic datum that does not fully account for processes like subsidence or sediment accretion. However, our manual measurements of water depth from LM-151 ($n = 473$) are robust for rSLR calculations because they are referenced directly to the seabed. These data are consistent with recently described sea level rise acceleration caused by

the compounding of wind driven Rossby waves over the Caribbean^{28,29}. This recent acceleration will likely be short-lived²⁹, but these rapid effects provide valuable empirical evidence of long-term effects of sea level rise on seagrasses rather than projected impacts alone^{36,54}. The 0.25 m increase in water depth observed at LM-151 would decrease available light for photosynthesis by 25–50%, sufficient to cause local extirpation and/or habitat shifts at this deep edge site.

Previous research has noted seagrasses as a potential “winner” compared to other coastal habitats under localized water depth changes⁴⁰. Likewise, under realistic future sea level rise scenarios⁵⁵ we predict that seagrass habitat can expand by up to 65 km² (Fig. 5). This value is an upper-bound and actual colonization may be significantly less because of factors like poor environmental conditions and shoreline hardening. Upper Laguna Madre has the largest potential for seagrass expansion into newly submerged lands in the Gulf of Mexico because it is bounded by undeveloped shorelines suitable for seagrass growth (53% of shorelines are suitable; Table S2). But the favorable situation in Laguna Madre is not reflected on most shorelines in the US because they have become increasingly artificially hardened³³ or are otherwise unsuitable for seagrass colonization. Currently, marshes represent a large source of uncertainty as potential seagrass habitat because they may or may not keep pace with sea level rise by maintaining sufficiently high accretion rates⁵⁶. In Texas, 41–64% (242–378 km) of the shoreline that incorporates seven large estuarine systems is unsuitable for seagrass colonization. Across the United States, hardened structures have removed 21,400 km of potential seagrass habitat and this number will continue to grow³³.

Globally, the trend of shoreline hardening is expected to continue and become exacerbated under future scenarios of stronger storms, higher erosion, and deeper waters³³. Although seagrasses within Laguna Madre are likely more resilient to continued sea level rise despite localized-rapid losses, the fate of other meadows within the Western Gulf of Mexico and elsewhere remains unknown. Worldwide, we estimate that over 14,000 km² of seagrass meadows live in turbid waters equivalent to Upper Laguna Madre ($K_d > 1$), suggesting they may also be sensitive to SLR (Table 1). These include over 50% of the seagrass meadows in the Netherlands, Poland, Sweden, Denmark, Canada, Senegal, Germany, and Norway. Seagrasses that occur in waters of high water transparency will also be lost because deep edge populations in these systems will switch from sufficient to insufficient light availability. Global seagrass populations are already threatened by the increased frequency of major storm events, eutrophication, fungal infections, algal blooms, and temperature extremes^{13,14}. Accelerated rises in sea level are yet another perturbation that displaces functional seagrass communities with unvegetated sediments that further compromise the productivity and integrity of coastal ecosystems worldwide through loss of both habitat and carbon sequestration potential is lost.

Methods

Site and monitoring description. The western Gulf of Mexico contains numerous estuarine systems including Laguna Madre, a unique hypersaline lagoon, which contains over 70% of Texas's 900 km² of seagrass meadows⁵⁷. Broadly, the system is divided into two regions (Upper and Lower) by a large tidal flat. Here, we are conducting seagrass monitoring efforts within the Upper Laguna Madre (ULM) that is bordered by Corpus Christi (TX) on the western shore and Padre Island National Seashore on the eastern (Fig. 1). Four seagrasses are found within ULM: (*Halodule wrightii*, *Halophila engelmannii*, *Ruppia maritima*, and *Syringodium filiforme*). ULM is bisected by the Gulf Intercoastal Waterway system, but either side is dominated by shallow (< 2 m) seagrass meadows.

Table 1 Areal coverage of global seagrass meadows⁶⁴ classified using remotely-sensed K_d values³⁵ based on susceptibility to sea level rise ($K_d > 1$).

Country	$K_d < 1$ (km ²)	$K_d > 1$ (km ²)	% $K_d < 1$	% $K_d > 1$
TOTAL	622017	14773	98	2
United States	11829	2852	81	19
Mexico	24101	2161	92	8
Senegal	1174	1775	40	60
Ukraine	9878	1727	85	15
Nigeria	16035	1317	92	8
Cuba	11662	1305	90	10
Australia	59546	881	99	1
Denmark	57	630	8	92
Philippines	13612	629	96	4
Germany	464	489	49	51
Sierra Leone	8192	278	97	3
Canada	62	158	28	72
OTHER	465405	572	—	—

A long-term seagrass monitoring station “LM-151” (27.35 N, 97.37 W) was established in 1989 within Padre Island National Seashore to track changes in a deep edge population of *Halodule*⁴⁶. Annual Tier-2 sampling of ULM began in 2011 across 144 stations in the ULM to assess broad-scale changes in seagrass populations. Details of the LM-151 sampling are provided below, whereas Tier-2 methods have been described previously⁴⁴. Data for the Tier-2 and LM-151 monitoring programs are available online^{58,59}.

Water quality measurements. Near-continuous underwater measurements of canopy-level photosynthetically active radiation (PAR) began at LM-151 in 1989 using a LI-193SA spherical (4π) quantum sensor connected to a LI-1000 datalogger (LI-COR Inc., Lincoln, Nebraska, USA)⁴⁶. Measurements were taken every minute and integrated over the hour before logging. Average daytime irradiance (ADI) was calculated by taking the monthly mean of daily averaged irradiance values between sunrise and sunset. This metric was chosen for analysis to minimize daily light variability and reflect growing conditions. A thin, optically clear plastic covering was placed over the sensor and replaced every 2–4 wk to reduce biofouling. During these maintenance trips, water temperature, conductivity (converted to salinity), pH, and dissolved oxygen were typically measured using a YSI-6920 datasonde (YSI, Yellow Springs, OH). Total suspended solids in the water column were quantified by measuring the dry filtrate from a 1L seawater sample retained on a pre-combusted $0.7\mu\text{m}$ glass fiber filter. Water depth was measured using a marked PVC pole. Additionally, Secchi depth was measured by lowering a black and white Secchi disk until no longer visible or the bottom was reached. Multiple measurements of environmental parameters taken within a month were averaged for analysis. Concentrations of ammonium and dissolved inorganic nitrogen were measured from replicate water samples following standard protocols⁶⁰.

Biological sampling. At LM-151, four biomass samples were taken haphazardly every 3–6 months. At each position, a PVC corer was pressed 30 cm into the sediment to collect aboveground and belowground tissues. The number of shoots in each sample were counted for each species before tissues were segmented into photosynthetic (aboveground) and non-photosynthetic (belowground) portions in the lab, dried, and massed. All values were averaged and standardized to m^{-2} coverage. Estimates of epiphytic algal biomass are made from separate leaf samples ($n = 3-6$) by scraping a known leaf area. The material is then collected and retained on pre-weighed glass fiber filters and dried

at 60 °C for determination of dry weight biomass. Data was collected at additional sites along the Texas coast for comparison⁶¹.

Data analysis and statistical modeling. Data analysis and visualization primarily used R (v 4.2.1), but ArcGIS Pro was used for mapping, inverse distance weighted interpolation, and areal calculations of spatial data (v 3.0.2). Locally estimated scatterplot smoothing (LOESS) lines were added to plots of environmental variables to aid in visualization of long-term trends. The relationship between water depth and the presence of seagrass at Tier-2 sampling locations was explored through hierarchical clustering of yearly water depth measurements. Data were scaled such that $\bar{x} = 0$, $\sigma = 1$ before a pairwise Euclidean distance matrix was generated for clustering through Ward’s method. Seagrass presence data were sorted according to match this clustering scheme.

General additive models (GAMs) were constructed using the mgcv package to evaluate the statistical relationship between biological and environmental parameters because of the non-linear nature of the parameters. The model basis functions were adjusted from their default values until smoothing was adequate, p-values were non-significant, and effective degrees of freedom did not significantly change. Various model families were tested, but assessment of model diagnostics led us to use the gamma distribution to assess environmental effects on seagrass biomass and binomial with a logit link function for seagrass presence. Aboveground biomass was chosen as the response variable because of greater data coverage than shoot density and strong correlation to belowground biomass. Water depth was the only explanatory variable tested for Tier-2 data because it is less sensitive to variations in weather or time of day and directly links to our a priori hypotheses. Biomass models were limited by the number of explanatory variables that could be added, so non-significant factors or those with low power were removed.

Coastwide sea level rise assessment. To determine statewide rates of relative sea level rise, we acquired data from 54 stations across the coast referenced to NAVD88⁶². We queried data from 1/1/1990 to 12/31/2022, but data coverage varied by station. Data was split into pre- and post-2014 sections for analysis to understand how rates may have changed following the loss of *Syringodium* in 2014. For each section, we used linear regression of daily maximum tidal heights over time to calculate relative sea level rise if at least 5 years of data existed. Non-significant slopes ($p > 0.05$) were assumed to be 0. For comparison, monthly averaged water depth measurements from LM-151 were analyzed in the same fashion.

Seagrass habitat change. To evaluate seagrass habitat change under future sea level rise we considered three scenarios of rSLR by 2050 for the Western Gulf of Mexico⁵⁵: best-case (+0.29m), intermediate/current-case (+0.37m), and worst-case (+0.49m). Under each scenario, we calculated the areal extent of land that would be submerged by each water depth increase and seafloor that would become unsuitable for seagrass growth. To estimate newly submerged habitat, 1-m resolution digital elevation models (DEM) were used to construct high-resolution shoreline topographic maps⁶². Next, the current shoreline position was estimated by calculating the mean sea level at Bird Island Basin tidal gauge (#8776139) during DEM acquisition⁶³. Increases in water depth were assessed using the 2018 water depth data generated by Tier-2 sampling to be specific for seagrass meadows, have moderate spatial resolution, and align with the DEM acquisition year. We chose a threshold of 1.5 m to represent unsuitable seagrass habitat, because meadows at this depth within Laguna Madre have less biomass and reduced presence probability (see results).

Reporting summary. Further information on research design is available in the Nature Portfolio Reporting Summary linked to this article.

Data availability

All seagrass monitoring data generated by this project have been deposited into publicly available repositories (<https://doi.org/10.25921/w3c1-sx54>; <https://www.ncei.noaa.gov/archive/accession/0181898>; <https://doi.org/10.5281/zenodo.10198512>). Additional datasets (e.g., shoreline suitability) were used, but are freely available from their respective publishers^{57,62–65}.

Received: 24 July 2023; Accepted: 23 January 2024;

Published online: 19 February 2024

References

- Larkum, A. W. D., Waycott, M. & Conran, J. G. *Evolution and Biogeography of Seagrasses*, 3–29 (Springer International Publishing, Cham, 2018). https://doi.org/10.1007/978-3-319-71354-0_1.
- McKenzie, L. J. et al. The global distribution of seagrass meadows. *Environ. Res. Lett.* **15**, 074041 (2020).
- Fong, P. & Harwell, M. A. Modeling seagrass communities in tropical and subtropical bays and estuaries: a mathematical model synthesis of current hypotheses. *Bull. Mar. Sci.* **54**, 757–781 (1994).
- Lee, K.-S., Park, S. R. & Kim, Y. K. Effects of irradiance, temperature, and nutrients on growth dynamics of seagrasses: a review. *J. Exp. Mar. Biol. Ecol.* **350**, 144–175 (2007).
- Mtwana Nordlund, L., Koch, E. W., Barbier, E. B. & Creed, J. C. Seagrass ecosystem services and their variability across genera and geographical regions. *PLoS ONE* **11**, 1–23 (2016).
- Costanza, R. et al. The value of the world's ecosystem services and natural capital. *Nature* **387**, 253–260 (1997).
- Duarte, C. M. et al. Seagrass community metabolism: assessing the carbon sink capacity of seagrass meadows. *Glob. Biogeochem. Cycles* **24** (2010).
- Kennedy, H. et al. Seagrass sediments as a global carbon sink: Isotopic constraints. *Global Biogeochem. Cycles* **24** (2010).
- Mazarrasa, I. et al. Seagrass meadows as a globally significant carbonate reservoir. *Biogeosciences* **12**, 4993–5003 (2015).
- Fourqurean, J. W. et al. Seagrass ecosystems as a globally significant carbon stock. *Nat. Geosci.* **5**, 505–509 (2012).
- Yingchun, L., Guirui, Y., Qiufeng, W. & Yangjian, Z. Huge carbon sequestration potential in global forests. *J. Resour. Ecol.* **3**, 193–201 (2012).
- Macreadie, P. et al. Vulnerability of seagrass blue carbon to microbial attack following exposure to warming and oxygen. *Sci. Total Environ.* **686**, 264–275 (2019).
- Orth, R. J. et al. A global crisis for seagrass ecosystems. *BioScience* **56**, 987–996 (2006).
- Waycott, M. et al. Accelerating loss of seagrasses across the globe threatens coastal ecosystems. *Proc. Natl Acad. Sci. USA* **106**, 12377–12381 (2009).
- Short, F. T. et al. Extinction risk assessment of the world's seagrass species. *Biol. Conserv.* **144**, 1961–1971 (2011).
- Onuf, C. Seagrass responses to and recovery from seven years of brown tide. *Pacific Conserv. Biol.* **5**, 306–313 (1999).
- Bestler, K. Effects of pesticides on seagrass beds. *Helgoland Marine Res.* **54**, 95–98 (2000).
- Sullivan, B. K., Sherman, T. D., Damare, V. S., Lilje, O. & Gleason, F. H. Potential roles of *Labyrinthula* spp. in global seagrass population declines. *Fungal Ecol.* **6**, 328–338 (2013).
- Hall, M. O., Furman, B. T., Merello, M. & Durako, M. J. Recurrence of *Thalassia testudinum* seagrass die-off in Florida Bay, USA: initial observations. *Mar. Ecol. Prog. Ser.* **560**, 243–249 (2016).
- Rodemann, J. R. et al. Impact of extreme disturbances on suspended sediment in Western Florida Bay: Implications for seagrass resilience. *Front. Mar. Sci.* **8** <https://www.frontiersin.org/articles/10.3389/fmars.2021.633240> (2021).
- Short, F. T. et al. Seagrassnet monitoring across the Americas: case studies of seagrass decline. *Mar. Ecol.* **27**, 277–289 (2006).
- Strydom, S. et al. Too hot to handle: Unprecedented seagrass death driven by marine heatwave in a world heritage area. *Glob. Change Biol.* **26**, 3525–3538 (2020).
- Marbà, N., Arthur, R. & Alcoverro, T. Getting turfed: the population and habitat impacts of *Lophocladia lallemandii* invasions on endemic *Posidonia oceanica* meadows. *Aquatic Botany* **116**, 76–82 (2014).
- Francoeur, P., Ganteaume, A. & Poulain, M. Effects of boat anchoring in *Posidonia oceanica* seagrass beds in the Port-Cros National Park (North-Western Mediterranean Sea). *Aquat. Conserv.: Mar. Freshwater Ecosyst.* **9**, 391–400 (1999).
- Duarte, C. M. Seagrass depth limits. *Aquatic Botany* **40**, 363–377 (1991).
- Lee, K.-S. & Dunton, K. H. Diurnal changes in pore water sulfide concentrations in the seagrass *Thalassia testudinum* beds: the effects of seagrasses on sulfide dynamics. *J. Exp. Mar. Biol. Ecol.* **255**, 201–214 (2000).
- Onuf, C. P. Seagrasses, dredging and light in Laguna Madre, Texas, USA. *Estuar. Coast. Shelf Sci.* **39**, 75–91 (1994).
- Dangendorf, S. et al. Persistent acceleration in global sea-level rise since the 1960s. *Nat. Clim. Change* **9**, 705–710 (2019).
- Dangendorf, S. et al. Acceleration of US Southeast and Gulf coast sea-level rise amplified by internal climate variability. *Nat. Commun.* **14**, 1935 (2023).
- Liu, Y., Li, J., Fasullo, J. & Galloway, D. L. Land subsidence contributions to relative sea level rise at tide gauge Galveston Pier 21, Texas. *Sci. Rep.* **10**, 17905 (2020).
- Milliner, C. et al. Tracking the weight of Hurricane Harvey's stormwater using GPS data. *Sci. Adv.* **4**, eaau2477 (2018).
- Haley, M., Ahmed, M., Gebremichael, E., Murgulet, D. & Starek, M. Land subsidence in the Texas Coastal Bend: Locations, rates, triggers, and consequences. *Remote Sens.* **14**, 192 (2022).
- Gittman, R. K. et al. Engineering away our natural defenses: an analysis of shoreline hardening in the US. *Front. Ecol. Environ.* **13**, 301–307 (2015).
- Lee, Z.-P. et al. Diffuse attenuation coefficient of downwelling irradiance: an evaluation of remote sensing methods. *J. Geophys. Res.: Oceans* **110** (2005).
- Ocean Biology Processing Group of the National Aeronautics and Space Administration. Aqua-MODIS Diffuse Attenuation Coefficient Mission Composite https://oceandata.sci.gsfc.nasa.gov/cgi/getfile/AQUA_MODIS_20020704_20230430.L3b.CU.KD.nc (2023).
- Saunders, M. I. et al. Coastal retreat and improved water quality mitigate losses of seagrass from sea level rise. *Glob. Change Biol.* **19**, 2569–2583 (2013).
- del Barrio, P. et al. Modeling future scenarios of light attenuation and potential seagrass success in a eutrophic estuary. *Estuar. Coast. Shelf Sci.* **149**, 13–23 (2014).
- Keyzer, L. et al. The potential of coastal ecosystems to mitigate the impact of sea-level rise in shallow tropical bays. *Estuar. Coast. Shelf Sci.* **246**, 107050 (2020).
- Kim, S. H., Kim, J. W., Kim, Y. K. & Lee, K.-S. Growth responses of the intertidal seagrass *Zostera japonica* to manipulated sea level rise conditions. *Bull. Mar. Sci.* **94**, 1379–1393 (2018).
- Albert, S. et al. Winners and losers as mangrove, coral and seagrass ecosystems respond to sea-level rise in Solomon Islands. *Environ. Res. Lett.* **12**, 094009 (2017).
- Pergent, G. et al. Dynamic of *Posidonia oceanica* seagrass meadows in the northwestern mediterranean: Could climate change be to blame? *Comptes rendus biologiques* **338**, 484–493 (2015).
- Williams, S. L. Experimental studies of caribbean seagrass bed development. *Ecol. Monogr.* **60**, 449–469 (1990).
- Gallegos, M. E., Merino, M., Rodriguez, A., Marbà, N. & Duarte, C. M. Growth patterns and demography of pioneer Caribbean seagrasses *Halodule wrightii* and *Syringodium filiforme*. *Mar. Ecol. Prog. Ser.* 99–104 (1994).
- Wilson, S. S. & Dunton, K. H. Hypersalinity during regional drought drives mass mortality of the seagrass *Syringodium filiforme* in a subtropical lagoon. *Estuaries and Coasts* **41**, 855–865 (2018).
- Dunton, K. H. & Tomasko, D. A. In situ photosynthesis in the seagrass *Halodule wrightii* in a hypersaline subtropical lagoon. *Mar. Ecol. Prog. Ser.* 281–293 (1994).
- Dunton, K. Seasonal growth and biomass of the subtropical seagrass *Halodule wrightii* in relation to continuous measurements of underwater irradiance. *Mar. Biol.* **120**, 479–489 (1994).
- Barber, B. J. & Behrens, P. J. Effects of elevated temperature on seasonal in situ leaf productivity of *Thalassia testudinum* Banks ex König and *Syringodium filiforme* Kützinger. *Aquatic Botany* **22**, 61–69 (1985).
- Major, K. M. & Dunton, K. H. Photosynthetic performance in *Syringodium filiforme*: seasonal variation in light-harvesting characteristics. *Aquatic Botany* **68**, 249–264 (2000).
- Dunton, K. H. Photosynthetic production and biomass of the subtropical seagrass *Halodule wrightii* along an estuarine gradient. *Estuaries* **19**, 436–447 (1996).
- Uy, W. *The interactive effect of shading and sediment conditions on growth and photosynthesis of two seagrass species, Thalassia hemprichii and Halodule uninervis*. Ph.D. thesis, Wageningen University (2001).
- Kaladharan, P. & Anasu Koya, A. Shrinking seagrass meadows observations from four lagoons of Lakshadweep Archipelago. *J. Mar. Biol. Assoc. India* **61**, 47–51 (2019).
- Short, F. T. & Short, C. A. The seagrass filter: Purification of estuarine and coastal waters. In *The Estuary as a Filter*, 395–413 (Elsevier, 1984).
- Bulmer, R. H., Townsend, M., Drylie, T. & Lohrer, A. M. Elevated turbidity and the nutrient removal capacity of seagrass. *Front. Mar. Sci.* **5**, 462 (2018).

54. Valle, M. et al. Projecting future distribution of the seagrass *Zostera noltii* under global warming and sea level rise. *Biol. Conserv.* **170**, 74–85 (2014).
55. Sweet, W. V. et al. *Global and Regional Sea Level Rise Scenarios for the United States: Updated Mean Projections and Extreme Water Level Probabilities along US Coastlines* (National Oceanic and Atmospheric Administration, 2022).
56. Kirwan, M. L., Temmerman, S., Skeehean, E. E., Guntenspergen, G. R. & Fagherazzi, S. Overestimation of marsh vulnerability to sea level rise. *Nat. Clim. Change* **6**, 253–260 (2016).
57. Office for Coastal Management. Seagrasses <https://www.fisheries.noaa.gov/inport/item/56960> (2023).
58. Dunton, K. et al. Seagrass canopy height, water depth, chlorophyll-a concentration and other plant and water quality indicators in Coastal Waters of Texas (NCEI Accession 0181898) <https://www.ncei.noaa.gov/archive/accession/0181898> (2023).
59. Dunton, K., Jackson, K., Schonberg, S. & Capistrant-Fossa, K. Seagrass density and biomass, water depth, dissolved oxygen, ammonium, dissolved inorganic nitrogen, suspended solids, water temperature, salinity, irradiance, pH in Laguna Madre Texas from 1989-03-24 to 2022-06-23 (NCEI Accession 0282643) <https://www.ncei.noaa.gov/archive/accession/0282643> (2023).
60. Parsons, T. R., Maita, Y. & Lalli, C. M. *A Manual of Chemical and Biological Methods for Seawater Analysis*. (Pergamon Press, 1984). <https://repository.oceanbestpractices.org/handle/11329/2043>.
61. Capistrant-Fossa, K. & Dunton, K. Algal Epiphyte Biomass from Seagrass Tissue Along the South Texas Coast (2011–2021) <https://doi.org/10.5281/zenodo.10198512> (2023).
62. U.S. Geological Survey. 3d elevation program 1-meter resolution digital elevation model <https://www.usgs.gov/3d-elevation-program> (2023).
63. National Oceanic and Atmospheric Administration. Tides and Currents <https://tidesandcurrents.noaa.gov/stations.html?type=Water+Levels> (2023).
64. UNEP-WCMC & Short, F. Global distribution of seagrasses (version 7.1) (2021).
65. Texas General Land Office. Environmental Sensitivity Index Shoreline <https://www.glo.texas.gov/land/land-management/gis/index.html> (2023).

Acknowledgements

Over three decades of seagrass monitoring would not have been possible without the numerous students, technicians, and scientists of the Dunton Lab including Kim Jackson, Susan Schonberg, Lisa Young, and Victoria Congdon. We are thankful for our major monitoring supporters including Texas Parks & Wildlife, Texas Commission on Environmental Quality, Texas General Land Office, Padre Island National Seashore, and the Texas Coastal Bend Bays & Estuaries Program. Major funding for this program was provided by the National Park Service (Gulf Coast Inventory & Monitoring Network; Padre Island National Seashore) and the Texas Coastal Bend Bays & Estuaries Program (Water and Sediment Quality Implementation Team). This publication was funded in part through a grant from the Texas General Land Office (GLO) providing Gulf of

Mexico Energy Security Act of 2006 funding made available to the State of Texas and awarded under the Texas Coastal Management Program. The views contained herein are those of the authors and should not be interpreted as representing the views of the GLO or the State of Texas.

Author contributions

KHD designed and acquired funding for both monitoring programs, KHD and KACF performed fieldwork, KACF performed data quality assurance/control, archiving, and statistical analysis. KACF and KHD wrote and revised the manuscript.

Competing interests

The authors declare no competing interests.

Additional information

Supplementary information The online version contains supplementary material available at <https://doi.org/10.1038/s43247-024-01236-7>.

Correspondence and requests for materials should be addressed to Kyle A. Capistrant-Fossa.

Peer review information *Communications Earth & Environment* thanks Christopher Patrick, Prama Wicaksono and the other, anonymous, reviewer(s) for their contribution to the peer review of this work. Primary Handling Editors: Christopher Cornwall, Joe Aslin, Clare Davis and Martina Grecequet. A peer review file is available.

Reprints and permission information is available at <http://www.nature.com/reprints>

Publisher's note Springer Nature remains neutral with regard to jurisdictional claims in published maps and institutional affiliations.



Open Access This article is licensed under a Creative Commons Attribution 4.0 International License, which permits use, sharing, adaptation, distribution and reproduction in any medium or format, as long as you give appropriate credit to the original author(s) and the source, provide a link to the Creative Commons licence, and indicate if changes were made. The images or other third party material in this article are included in the article's Creative Commons licence, unless indicated otherwise in a credit line to the material. If material is not included in the article's Creative Commons licence and your intended use is not permitted by statutory regulation or exceeds the permitted use, you will need to obtain permission directly from the copyright holder. To view a copy of this licence, visit <http://creativecommons.org/licenses/by/4.0/>.

© The Author(s) 2024